

Investigating young water fractions in a small Mediterranean mountain catchment: both precipitation forcing and sampling frequency matter

Francesc Gallart¹, María Valiente², Pilar Llorens³, Carles Cayuela⁴, Matthias Sprenger⁴, and Jérôme Latron⁵

¹CSIC

²University of the Basque Country - Bizkaia Campus

³Institute of Environmental Assessment and Water Research. CSIC

⁴IDAEA

⁵IDAEA-CSIC

May 5, 2020

Abstract

The young water fraction (F_{yw}), the proportion of water younger than 2-3 months, was investigated in soil-, ground- and stream waters in the 0.56 Km² sub-humid Mediterranean Can Vila catchment. Rain water was sampled at 5-mm rainfall intervals. Mobile soil water and groundwater were sampled fortnightly, using suction lysimeters and two shallow wells, respectively. Stream water was dynamically sampled at variable time intervals (30 minutes to 1 week), depending on flow. A total of 1,529 ¹⁸O determinations obtained during 58 months were used. The usual hypothesis of rapid evapotranspiration of summer rainfall could not be maintained, leading to discard the use of an “effective precipitation” model. Soil mobile waters had F_{yw} up to 34%, while in ground and stream were strongly related to water table and discharge variations, respectively. In stream waters, due to the highly skewed flow duration curve, the flow-averaged young water fraction (F^*_{yw}) was 22.6%, whereas the time-averaged F_{yw} was 6.2%. Nevertheless, both F^*_{yw} and its exponential discharge sensitivity (S_d) showed relevant changes when different 12-month sampling periods were investigated. The availability of S_d and a detailed flow record allowed us to simulate the young water fraction that would be obtained with a virtual thorough sampling (F^{**}_{yw}). This showed that underestimation of F^*_{yw} is associated with missing the sampling of highest discharges and revealed underestimations of F^*_{yw} by 25% for the dynamic sampling and 66% for the weekly sampling. These results confirm that the young water fraction and its discharge sensitivity are metrics that depend more on precipitation forcing than on physiographic characteristics, so the comparisons between catchments should be based on mean annual values and inter-annual variability. They also support the dependence of the young water fraction on the sampling rate and show the advantages of flow-weighted F^*_{yw} . Water age investigations should be accompanied by the analysis of flow duration curves. In addition, the simulation of F^{**}_{yw} is proposed as a method for checking the adequacy of the sampling rate used.

1. Introduction

Since the pioneering study by Maloszewski, Rauert, Stichler & Herrmann (1983), the comparison between the seasonal variation of stable isotopes (²H and ¹⁸O) of precipitation and stream waters, applying either the convolution integral or sinusoid fitting, has been used to investigate the turnover time of water in catchments. Mean transit times (MTT) and transit time distributions (TTD) of catchment waters have been intensively investigated for over three decades using these methods (McGuire & McDonnell, 2006), despite limitations of

stable isotopes for water fractions that are more than a few years old (Stewart, Morgenstern & McDonnell, 2010; Stewart, Morgenstern, McDonnell & Pfister, 2012).

More recently, Kirchner (2016a) demonstrated that MTT determinations with these methods may be inadequate, especially when waters of different ages mix along their flow paths within catchments. Kirchner (2016a) proposed an alternative travel-time metric, the ‘fraction of young water’ (F_{yw}), defined as the portion of water that is younger than a threshold age. This fraction can be robustly estimated for a wide range of TTDs, with a threshold age ranging between two and three months, depending on the TTD. Young water fractions have been subject to several developments and applications recently, leading to the opening of numerous questions regarding the methods’ specifics, the quality of the F_{yw} estimates, and their relationship to hydrological processes. We can group these questions to four main topics frequently mentioned in the literature: the water recharge assumption, the identifiability of catchment F_{yw} , the issue of sampling rate and the behaviour of mountain catchments. We briefly outline the four issues below:

- How must summer precipitation be taken into account (i.e., effective precipitation) for F_{yw} and MTT determinations when using stable isotopes of water?

In a seasonal climate, precipitation (or throughfall) is more enriched in heavy water isotopes during summer than during winter (Allen *et al.* 2019a), while evapotranspirative demand is higher in summer than in winter. Consequently, isotopically enriched summer precipitation might be less likely to recharge the storage of a hydrological system, since evaporation is more likely to be sourced from summer rainfall. As a result, the isotope ratios of the infiltrating rain becoming recharge (“effective rainfall”) will probably be biased towards cold/dormant season rainfall (Jasechko *et al.* 2014), and its seasonal oscillation will be more attenuated than that of precipitation. However, there is no consensus on how this issue (“the recharge assumption“ in McGuire & McDonnell, 2006) is to be handled.

A first approximation of effective rainfall is weighting the sampled isotope ratio by ‘precipitation minus evapotranspiration’ rather than precipitation. This is habitually obtained using a conceptual soil water-balance or rainfall loss (sub-) model before or at the beginning of the modelling exercise or data analysis (e.g. Dunn, McDonnell & Vaché, 2007; Lutz *et al.* 2018; Stewart *et al.* 2007; Stockinger *et al.* 2016; Weiler, McGlynn, McGuire & McDonnell, 2003). This approach assumes that evapotranspiration is composed of the latest rainfall, at the sampling/modelling time step. However, summer evapotranspiration may consume soil water that is several months old, as isotope data suggest (Allen *et al.* 2019b; Brooks, Barnard, Coulombe & McDonnell, 2010; Sprenger, Llorens, Cayuela, Gallart & Latron, 2019a), potentially overestimating evapotranspiration losses of summer precipitation.

A second approach accounts for the isotope ratio and age dynamics of the evapotranspiration flux: both are simulated with those of runoff to update the isotope ratio and age distributions of the catchment storage. This approach is for example used in the StorAge Selection (SAS) modelling (van de Velde *et al.* 2012; Benettin *et al.* 2017; Harman, 2015) and other flow tracking models (Soulsby *et al.* 2015; Soulsby, Birkel & Tetzlaff, 2016).

A third approach performs mass balance based equations of diverse flows and compartments (precipitation, runoff, groundwater, evapotranspiration) between seasons for assessing the share of precipitation in these partitions (Grabczak, Maloszewski, Rozanski & Zuber, 1984; Maloszewsky, Rauert, Stichler & Herrmann, 1992; Jasechko *et al.* 2014; Kirchner & Allen, 2020). The advantage of this approach is that it does not need assumptions (beyond the conservation of the tracers and a steady state or null balance of the storage) nor parameters, therefore its uncertainty is only related to the quality of observations (measurement accuracies of rainfall-runoff volumes and its isotope ratios) and to the differences of tracer concentrations between the various compartments.

Finally, some authors do not claim to take into account this possible effect and use the gross isotopic signature of precipitation waters (or throughfall or melting) as input to the hydrologic system (e.g. von Freyberg, Allen, Seeger, Weiler & Kirchner, 2018; Stockinger, Bogena, Lücke, Stump & Vereecken, 2019; Jacobs *et al.* 2018), although Lutz *et al.* (2018) refrained from considering evapotranspiration in the weighting of the isotope

values in precipitation because the used effective rainfall model showed minor differences between both signatures.

- Can F_{yw} be characterized as a catchment descriptor?

One of the expected applications of F_{yw} in catchments is its suitability as a metric for catchment intercomparison (Kirchner 2016a, b; von Freyberg *et al.*, 2018; Jasechko *et al.* 2016; Lutz *et al.* , 2018). Nevertheless, F_{yw} is basically non-stationary and climate factors seem to overwhelm catchment physiographic characteristics: F_{yw} is known to usually increase with stream discharge due to the activation of faster flow paths when the wetness of the catchment increases (Kirchner 2016a, b; von Freyberg *et al.* , 2018; Gallart *et al.*, 2019).

Consistent with this behaviour, F_{yw} was found in several studies to increase during wetter years (Bansah & Ali, 2019; Clow, Mast & Sickman, 2018; Remondi, Botter, Burlando & Fatichi, 2019; Wilusz, Harman & Ball, 2017; Zhang *et al.* , 2018) and in wetter catchments (von Freyberg *et al.* , 2018; Remondi *et al.* , 2017). The importance of rainfall intensity dynamics on catchment MTT or F_{yw} was also stressed by several authors (von Freyberg *et al.* , 2018; Soulsby, Piegat, Seibert & Tetzlaff, 2011, Remondi *et al.* , 2019; Wilusz *et al.* , 2017).

Furthermore, Stockinger *et al.* , (2019) showed that catchment F_{yw} was not only sensitive to (long-term) changes annual hydro-climatic variations, but also to (short-term) changes of the starting date of a sampling campaign.

- How sensitive is F_{yw} to sampling rate?

Although F_{yw} may be estimated from irregularly and sparsely sampled tracer time series (Kirchner, 2016a), Stockinger *et al.* . (2016) showed for the Erkensruhr catchment (41.7 km²) that F_{yw} almost halved and MTT doubled when the original daily or sub-daily data were aggregated to a weekly sampling rate. Several studies have shown that to obtain sound estimates of hydrological dynamics it is necessary to take samples at the corresponding time scales (Kirchner, Feng, Neal, & Robson, 2004; von Freyberg, Studer and Kirchner, 2017; Neal *et al.* , 2012). However, it remains to be tested what temporal sampling resolution is sufficient, accounting for cost efficiency, to cover the highly variable age distribution of stream water (Sprenger *et al.* , 2019b).

Yet, tracer concentrations must be weighted by the corresponding precipitation and streamflow volumes for their mass to be compared (Kirchner, 2016a). Walling (1988) provided classical examples of the issues related to both the representativeness of sediment sampling and the adequate flow-weighting of concentrations.

However, many of the F_{yw} and MTT studies are based on monthly to weekly sampling schemes designed from operational rather than hydrological constraints. Frequently, authors wonder about the representativeness of their samples, but detailed information on the flow regimes or the comparison with those sampled is rarely given. Hydrographs are scarce and flow duration curves are rarely discussed or shown. Mass-weighting of tracer concentrations is a normal procedure in precipitation but seldom applied for stream waters.

- Are F_{yw} values lower in mountainous catchments?

Several studies found that high-gradient or -elevation catchments have lower F_{yw} values or longer MTT (Jasechko *et al.* , 2016; Jasechko, Wassenaar & Mayer, 2017; Lutz *et al.* , 2018; Song *et al.* , 2017), whereas other studies found a converse relationship (Clow *et al.* , 2018; Zhang *et al.* , 2018) or no clear relationship (von Freyberg *et al.* , 2018; Soulsby *et al.* , 2011). Although von Freyberg *et al.* (2018) did not find significant relationships between F_{yw} and the elevation gradient in their 22 studied Swiss catchments, their median value was found to be consistent with Jasechko *et al.* 's (2016) observation that young water fractions tend to be smaller in steeper landscapes. Using monthly sampled water geochemistry, Frisbee *et al.* , (2011) found that groundwater contributions increased with increasing scale in mountainous drainage areas greater than 100 km² but decreased with increasing scale in headwater drainage areas smaller than 100 km². On the other hand, long-term weekly or bi-weekly stream water sampling in a high mountain 1.55 km² catchment showed a low (4.5%) contribution of groundwater to stream flow (Dwivedi *et al.* , 2018). Daily data in two

small (0.51 and 3.47 Km²) mountain catchments at Plynlimon (Wales) showed that MTTs were as short as 0.36 and 0.82 years respectively (Kirchner *et al.*, 2001). Yet, simulation exercises made at hourly and daily time scales, showed higher F_{yw} and shorter MTT values in steeper catchments irrespectively of the climate (Remondi *et al.*, 2019).

The more consolidated hypothesis is that mountain catchments tend to yield lower F_{yw} and longer MTT, contrarily to the intuition, attributed to the deeper infiltration of rain water (Jasechko *et al.*, 2016). Though, mountainous catchments are commonly considered to have fast hydrological responses to precipitation (Arnell, 1989), so the question arises whether mountain catchments have always been sampled at a temporal frequency appropriate to their hydrological dynamics for assessing sound F_{yw} values.

This paper aims to address the outlined research gaps by applying the recent F_{yw} developments to investigate the turnover of waters in diverse hydrological compartments of the small Can Vila research catchment (Vallcebre Research Catchments; Gallart, Llorens, Latron & Regüés, 2002; Llorens *et al.*, 2018). Our work contributes to the methodological development and understanding of F_{yw} by testing its application using weekly to sub-hourly precipitation and stream water samples along with fortnightly mobile soil and shallow ground waters samples. Our work further aims to shed light into the interpretation of F_{yw} by combining the results with the understanding of hydrological processes in a long-term research catchment. Thus, the objectives of this work are both to improve understanding of the hydrological functioning of the Can Vila catchment and to test the F_{yw} concept in an intensively investigated Mediterranean mountain environment.

2. Materials and Methods

2.1 Study area

The study was conducted in the Can Vila catchment (0.56 Km²), one of the sub-catchments of the Vallcebre research catchments (Llorens *et al.*, 2018) at the headwaters of the Llobregat River, about 130 km northeast of Barcelona, on the southern margin of the Pyrenees, Catalonia (42°12' N, 1°49' E).

In the Can Vila catchment, elevations range between 1,115 and 1,458 m above sea level. Slope gradients are moderate, with a mean value of 25.6% (Latron & Gallart, 2007), and have dominant north-east aspects. Before and during the 19th century, most of the hillslopes were deforested and terraced for agricultural purposes. The terraces are mostly 10 to 20 meters wide and limited by a stone wall up to 2 meters high, covering around half the area. Along with terraces, a network of artificial ditches was also built in order to prevent soil saturation and to convey surface runoff (Llorens, Latron & Gallart, 1992; Gallart, Llorens & Latron, 1994). During the second half of the 20th century the land was steadily abandoned. Following land abandonment, spontaneous forestation by *Pinus sylvestris* patches occurred (Poyatos, Latron & Llorens, 2003) and forest now covers 34% of the catchment. The remainder of the catchment is covered by pasture and meadows. The main channel is 1 to 2 m wide and is not deeply incised near the outlet.

The bedrock of the Can Vila catchment consists almost entirely of upper smectite-rich mudrocks with sandstone and gypsum layers of the continental Tremp formation (Upper Cretaceous-Paleocene), with the exception of the western part, where lacustrine micritic limestone appears almost vertically. This catchment, almost entirely on clayey bedrock, is considered to be totally watertight, with no noticeable deep percolation (Latron, Soler, Llorens & Gallart, 2008), although some local aquifers occur in sandstone and gypsum layers that feed small permanent sources within the catchment. Soils developed over mudrocks are predominantly of silt-loam texture. Topsoil is rich in organic matter (on average 4.1% from 0 to 55 cm below the ground surface) and well-structured, with high infiltration capacity in the upper 20 cm (Solé, Gallart, Pardini & Aringhieri, 1992), while hydraulic conductivity decreases rapidly at greater depth (Rubio, Llorens & Gallart, 2008). These soil conditions result in formation of shallow permanent aquifers over the impervious bedrock and some transient perched aquifers during major rainfall events. Soil water content is characterized by periods of marked deficit in summer and, though less pronounced, in winter. In summer, soil cracking occurs, which enhances infiltration capacity. Soil thickness varies greatly as a consequence of terracing, ranging from less than 50 cm in the inner part of terraces to more than 3 m in their outer part (Latron *et al.*, 2008). A small

part of the catchment (0.9%) is occupied by bare limestone and mudrock outcrops with little-developed badlands landforms.

Climate is defined as Mediterranean humid, with a marked water deficit in summer. Long-term (1988-2013) mean annual precipitation was 880 ± 200 mm (Llorens *et al.* , 2018), with on average 90 rainy days per year (Latron, Llorens & Gallart, 2009). Snowfall accounts for less than 5% in volume. The rainiest seasons are autumn and spring with mean rainfall above 100 mm/month in October, November and May (Latron & Gallart, 2008). Winter is the season with least rainfall, while in summer convective storms may produce significant rainfall inputs. The mean annual temperature is 9.1 °C at 1,260 m a.s.l. and mean potential annual evapotranspiration, calculated by the method of Hargreaves and Samani (1982), is 823 ± 26 mm. The isotopic signatures of meteoric water in Vallcebre are influenced by Western Mediterranean and Atlantic Ocean air masses. The weighted average isotope ratios for the study period between 2011 and 2016 were -44.14 ± 2.30 ($\delta^2\text{H}$), -7.17 ± 0.29 13.19 ± 0.51

The combined dynamics of rainfall and evapotranspiration favour the succession of wet and dry or very dry conditions in the catchment during the year (Latron & Gallart, 2007). Dry and very dry periods occur in winter and summer, respectively, whereas wet periods occur in spring and late autumn. Three types of runoff events were identified on the basis of hydrometric observations (Latron & Gallart, 2007; 2008). Intense rainfall events during summer induce flash floods with very low runoff coefficients, attributed to infiltration-excess overland flow on bare bedrock and badland areas. Second, during transitions from dry to wet conditions, more frequent and/or greater rainfall events induce larger runoff events with moderate runoff coefficients with long response times and relatively gentle recessions, attributed to a scattered pattern of perched soil saturation. Third, under wet conditions, moderate rainfall events induce large and lasting runoff events associated with rapid responses of the water table, attributed to overland flow on saturated areas and return flow. Flow in the Can Vila stream usually ceases for a few weeks during the summer each year, though remaining stagnant pools rarely become totally dry.

Two-component hydrograph separation studies using stable isotopes indicate that pre-event water contributed between 30% and almost 100% to total runoff, depending on antecedent moisture conditions, the extent of saturated areas within the catchment and precipitation characteristics (Latron, Roig-Planasdemunt, Llorens & Gallart, 2015; Cayuela *et al.* , 2019). During low to moderate-intensity rainfall events (winter, spring, autumn), pre-event water contribution was dominant (>90%). Conversely, during high-intensity summer storms, pre-event water contribution was lower (30% to 50%) and the response corresponded mostly to new water. Pre-event water contribution at the event scale decreases with increasing maximum rainfall intensity. In addition, pre-event water contribution and the maximum suspended sediment concentration observed at the outlet correlate negatively, which supports the view that summer floods are mainly caused by infiltration excess runoff generated on badlands and degraded areas of the catchment (Latron *et al.* , 2015).

The use of tritium to investigate the turnover of waters during low-flow conditions (Gallart *et al.*, 2016) has shown MTTs of nearly 5 years for shallow open groundwaters and 7.5 years for both stream base flow and a permanent spring near the centre of the catchment.

2.2 Data acquisition

2.2.1 Hydrological measurements and water sampling

Rainfall volumes for the period 2011-2017 were recorded at 5-minute steps with tipping-bucket rain gauge, located 1 m above the ground near the gauging station (Figure 1).

The depths to the water table at the VP01 and VP05 piezometers were recorded every 20 min with autonomous Micro-Diver sensors (Van Essen Instruments), subsequently corrected for atmospheric pressure changes.

Stream discharge was measured at the Can Vila (CV) gauging station, by means of a 90o V-notch weir with

a water pressure sensor (6542C-C, Unidata) connected to a data-logger (DT50, Data Taker). Mean water level values were recorded every 5 minutes and converted to discharge values with an established rating curve calibrated with manual discharge measurements (Latron & Gallart, 2008). Discharge values were originally expressed in L s^{-1} and converted, without time aggregation, into millimetres per day (mm d^{-1}) for comparison with other studies.

In the Can Vila catchment, waters for stable isotope ($\delta^{18}\text{O}$ and $\delta^2\text{H}$) analyses were sampled from rain and stream at one site at the catchment outlet, from groundwater at two sites (VP01 and VP05) and from mobile soil water at two sites (VL01 and VL02) (see Figure 1).

Rainfall isotope data corresponded to samples taken during two time periods between 2011 and 2017. The first period ran from May 2011 to July 2013 and the second, from May 2015 to November 2017. Two types of rain water samplers were used. A bulk rainfall sampler, consisting of a 180-mm diameter funnel connected to a 1 L plastic bottle with a pipe with a loop, provided information of the isotopic composition of rainfall on an approximately weekly basis. Rain water was further sampled automatically at 5 mm rainfall intervals with a sequential rainfall sampler, using an open collector (340 mm diameter) connected to an automatic water sampler (24 500-mL bottles, ISCO 2900). Both containers (bottle and sampler) were buried in the ground to avoid evaporation. The two sampling records were aggregated, (i.e., using the finest time interval available and removing duplicate samples) providing a data set of 464 rainfall isotopes samples.

As shown by Cayuela *et al.* (2019), the location of the rainfall sampling site at the lowest part of the Can Vila catchment means that the sampled isotope signature is more enriched than the average for the catchment. However, the isotopic enrichment of throughfall in the forested areas compensates for this effect. Consequently, no compensation of the isotopic signature in precipitation due to elevation effects was deemed necessary.

Soil mobile waters were sampled at two locations with a battery of low-suction cup lysimeters installed between 50 (2 lysimeters) and 100 (4 lysimeters) cm depth. The soil water sample at each location was a mixture of the water collected at different lysimeters and depths. Soil water was sampled weekly or fortnightly from May 2011 to July 2013 when water could be extracted. Over the study period, 63 samples from VL01 and 37 from VL02 were analysed for isotopic composition.

Groundwaters were sampled at two locations near the surface of the water table with a manual peristaltic pump, as electrical conductivity profiles conducted on several occasions showed no stratification of the waters. VP01 is a 2.06 m-deep piezometer lined with a 55 mm-diameter PVC tube, which is sealed for the upper 0.5 m to prevent entrance of surface waters and has open access below. VP05 is a 4.22 m-deep abandoned well. Its walls are covered by boulders, allowing water to flow throughout the full depth. Groundwater was sampled weekly or fortnightly from May 2011 to July 2013. A total of 36 samples were taken from the VP01 piezometer (that sometimes dried out) and 71 from the (permanent) VP05 well.

Stream water was sampled during two periods, from May 2011 to September 2013 and from late May 2015 to May 2016, using a sampling scheme designed for obtaining information for isotopic hydrograph separation (IHS) at the event scale (Cayuela *et al.*, 2019). Manual grab samples were taken weekly during visits and two automatic water samplers (24 1 L bottles, ISCO 2700) were operated by the data-logger. One sampler was scheduled to take a sample every 12 hours and the other was triggered when stream water level exceeded a certain threshold, taking samples at a higher rate when the water level rose than when it declined. Samples of little relevance to IHS such as those repeatedly taken during long recessions or base flows were discarded, reducing the total number of stream samples analysed for isotopic composition to 858 at the Can Vila outlet. The final sampling rate was between 30 minutes and 1 week, although there are some gaps due to the drying of the stream.

2.2.2 Isotopic analyses and pre-treatment

During the sampling periods, all samples were brought together once a week during field visits. Manual samples of stream, soil and groundwaters were directly collected in glass vials. The bottles of the automatic

rainfall and stream samplers were capped and transported to the laboratory under cold conditions, where two samples from every bottle were deposited in 3-ml glass vials. These vials were fully filled to avoid bubbles and sealed with plastic paraffin film to avoid fractionation caused by evaporation. For each sample a replica was prepared. All samples were stored at 3-4 °C prior to analysis.

-Stable isotopes of water (^{18}O and ^2H) were analysed by a Cavity Ring-Down Spectroscopy Picarro L2120-i isotopic water analyser at the Scientific and Technological Services of the University of Lleida. All isotope data were expressed in terms of δ -notation as parts per mile (calibrated to Vienna Standard Mean Ocean Water (V-SMOW) (Craig, 1961). Accuracy of the analyses, based on the repeated analysis of four reference water samples, was $< 0.1\delta^{18}\text{O}$ and $\delta^2\text{H}$, respectively. When samples contained organic compounds a post-processing correction was applied (Martín-Gómez *et al.* , 2015).

The isotopic signatures of the precipitation samples were weighted by their corresponding precipitation depths before further calculations. Furthermore, following frequent procedures (e.g. McGuire & McDonnell, 2006; Jasechko *et al.* , 2014; Lutz *et al.* , 2018), a soil water-balance model was used to estimate the effective precipitation (precipitation minus evapotranspiration) for weighting the isotopic signature of the waters entering the hydrological system, under the hypothesis that precipitation in the warmer months evaporates more and contributes less to the hydrological compartments than precipitation in the remaining months. For this purpose, the conceptual lumped Thornthwaite-Mather model (Steenhuis & van der Molen, 1986) was implemented at a weekly time step, after calibration with the flow records of the Can Vila catchment. This model was selected because it simulates the effective (runoff or recharge) water as the precipitation minus potential evapotranspiration that exceeds the remaining water retention capacity of the root zone. Water retained in the root zone is not transferred to runoff or recharge but just evapotranspired. This needs the simulation of both the water balance in the root zone and the actual evapotranspiration with a single calibrated parameter, thus providing a good balance between soundness and simplicity.

Nevertheless, as stated in the introduction, the hypothesis of rapid evapotranspiration of rainfall waters in summer may be questioned on the basis of recent research. Consequently, the hypothesis of the decreased hydrological role of summer precipitation was subject to two tests based on mass balance methods. The first test was proposed by Grabczak, Maloszewski, Rozanski & Zuber (1984) and further developed by Maloszewsky, Rauert, Stichler & Herrmann (1992) to estimate ρ , the relative contribution of summer precipitation to groundwaters (or any other hydrological compartment):

$$\rho = \frac{[\sum_W (P_i C_i) - C_{gw} \sum_W (P_i)]}{[C_{gw} \sum_S (P_i) - \sum_S (P_i C_i)]} \quad (1)$$

where ρ values higher or lower than unity reflect higher or lower contributions of summer rainfall to the hydrological storage, respectively; P represents precipitation; C represents the concentration of stable isotopes of water, along with the subscripts W for “winter” months (September to May), S for “summer” months (June to August) and gw denoting groundwaters or any other compartment under consideration. These different periods were selected in order to avoid the effect of the dominant equinoctial precipitation.

A second, more quantitative test analysed the partitioning of seasonal precipitation into runoff and evapotranspiration, according to Kirchner and Allen (2020). Following these authors, using mass balances, the splitting of seasonal precipitation into runoff can be assessed by:

$$\eta_{P_s \rightarrow Q} = \frac{Q}{P_s} \frac{\delta_Q - \delta_{P_w}}{\delta_{P_s} - \delta_{P_w}} \quad (2)$$

where $\eta_{P_s \rightarrow Q}$ represents the fraction of summer precipitation that eventually becomes streamflow. X is the annual runoff. P_s is the summer precipitation. δ represents the volume-weighted isotope signatures for the compartments denoted by the subscripts: Q for stream waters, P_w for winter precipitation and P_s for summer precipitation.

Furthermore, summer precipitation can be split into evapotranspiration and runoff, which are complementary. Thus, using the same notations, the fraction of runoff that derives from summer precipitation can be

calculated as:

$$f_{Q \leftarrow P_s} = \frac{\delta_Q - \delta_{P_w}}{\delta_{P_s} - \delta_{P_w}} \quad (3)$$

As both the isotope ratio of groundwater and its temporal variability varied with the water table level at VP05, two different approaches were implemented. First, the available record was divided into two sub-series: samples taken when water table level was deeper than 2.25 m were classified in the ‘deep’ group and samples corresponding to shallower water levels in the ‘shallow’ group. Second, an attempt was made to obtain a mass-averaged isotope ratio by weighting with the exponent of the water table level over its minimum value, used as a surrogate of groundwater flow (Latron & Gallart, 2008).

Stream water samples were taken at different frequencies and discharge regimes. Therefore, their isotopic signatures were flow-weighted to obtain mass-representative values (Kirchner, 2016a) and time-weighted for comparison with other studies (Jasechko *et al.*, 2016; von Freyberg *et al.*, 2018). In addition, following the methods proposed by Kirchner (2016b) and von Freyberg *et al.* (2018), the original record was divided into a set of sub-samples according to the respective discharge rates, in order to analyse the dependence of the young water fraction on the flow regime. Finally, for comparison with other studies that used weekly to monthly sampling rates, a subordinate sample set with a weekly rate was extracted from the original one.,

2.3 Young water fraction estimations

Following the methods and notations proposed by Kirchner (2016a), the seasonal amplitudes A and phases of the $\delta^{18}\text{O}$ signatures c of waters in precipitation, estimated recharge, stream, soil and groundwater in the catchment were estimated by non-linear fitting through the equation:

$$c = A \sin(2 \pi f t - \varphi) + k \quad (4)$$

where f (year⁻¹) is the frequency of the cycle ($f = 1$ for a seasonal cycle), t is time (years with decimal fractions) and k is the zero value or vertical shift of the sinusoid. In young water fraction studies, non-linear fitting methods that limit the influence of outliers are commonly used (e.g., Kirchner, 2016a; Stockinger *et al.*, 2016; von Freyberg *et al.*, 2018). In our case, the distribution of $\delta^{18}\text{O}$ in precipitation had less extreme values than a normal one (platykurtic, kurtosis $K = 1.0$), whereas in the stream water $\delta^{18}\text{O}$ distribution, the extreme values were much more important (leptokurtic, $K = 26.9$). Therefore, we decided to use least-squares fitting, as the outliers might contain hydrologically relevant information.

Subsequently, the F_{yw} for the waters investigated (i.e., stream water, groundwater, mobile soil water) was estimated as the ratio between the amplitudes of the isotope ratios in these waters and the amplitude of precipitation (or recharge) waters:

$$F_{yw} = \frac{A_x}{A_p} \quad (5)$$

where the p and x subscripts represent the precipitation and investigated waters, respectively.

Following the notation used by von Freyberg *et al.* (2018), we designated F_{yw} as the time-weighted young water fraction and F_{yw}^* as the flow-weighted young water fraction.

Although the TTD of waters was not an objective of this study, research into the young water fractions for a set of flow regimes cast doubt on the potential role of the threshold age $\tau_{\psi\omega}$ of these fractions. For this purpose, the shape factor α of the likely gamma distribution for every one of the flow regime sub-samples was estimated by iteratively solving the implicit equation (Kirchner, 2016a):

$$\varphi_s - \varphi_p = \alpha \arctan \left(\sqrt{\left(\frac{A_s}{A_p}\right)^{\frac{-2}{\alpha}} - 1} \right) \quad (6)$$

where the subscripts s and p correspond to the stream and precipitation, respectively, and A and φ represent sinusoid amplitudes and phase shifts, respectively. Once the shape factor α was obtained, the corresponding

threshold ages $\tau_{\psi\omega}$ of the young water fractions were calculated by means of the following second-order polynomial fit (Kirchner, 2016a):

$$\frac{\tau_{yw}}{T} \approx 0.0949 + 0.1065 \alpha - 0.0126 \alpha^2 (7)$$

Finally, the dependence of the young water fraction on stream discharge or its discharge sensitivity was investigated by two methods. First, we estimated F_{yw} for different quantiles of the flow regime (similar to Figure 7 in von Freyberg et al., 2018). Second, we assumed that F_{yw} was not a fixed value but that it increased with discharge up to a limit value of 1, following an exponential-type equation (Gallart et al., 2019):

$$F_{yw}(Q) = 1 - (1 - F_0) \exp(-Q S_d) (8)$$

where F_0 (1) is the Y-intercept or virtual F_{yw} for $Q = 0$ and S_d (unit of Q^{-1}) is the discharge sensitivity metric. These metrics can be obtained by non-linear fitting of the equation (Gallart et al., 2019):

$$c_s(t) = A_P [1 - (1 - F_0) \exp(-Q(t) S_d)] \sin(2 \pi f t - \varphi_S) + k_S (9)$$

where subscripts s and p are the same as in Eq. (6).

In a first exercise, F_{yw} and its discharge sensitivity were investigated in stream waters by applying Eqs. (4),(5) and (9) in the full record available, lumping the 58 months as in a single year. In a subsequent step, several 12-month time windows of both precipitation and stream waters were selected for the application of these equations, in order to investigate the relevance of the precipitation forcing.

Finally, although the 858 water samples/discharge values taken at variable time steps could be expected to provide a reasonable picture of the stream dynamics at Can Vila, a further test was conducted by applying Eq. (8) to the 228,095 5-minute discharge readings available for the sampling periods. The flow-averaging of the resulting $F_{yw}(Q)$ simulations for all these readings provided us with a hypothetically fully-sampled flow-weighted young water fraction that we labelled F_{yw}^{**} .

Statistics were performed with the help of the statistical package SPSS (IBM Corp.) using a Levenberg-Marquardt algorithm for non-linear estimations. Uncertainties were mostly expressed as standard errors except for the threshold ages $\tau_{\psi\omega}$ where the uncertainties were expressed as 90% confidence limits, using 10,000 Monte Carlo solutions of Eq. (6). Error propagation was estimated using Gaussian methods, following the guidelines proposed by Kirchner & Allen (2020, supplement) particularly for end-member mixing and splitting, as well as calculation of weighted averages. Statistical significance was set at $p < 0.01$ and marginal significance was set at $p < 0.05$, although the probability of the null hypothesis is sometimes indicated. The notation (1) after a variable name indicates that this variable is a dimensionless number.

3. Results

3.1 Isotopic characteristics of the sampled waters

During the study period, annual precipitation was similar to the long term mean value (860 mm/year) with 12-months minimum of 671 and maximum of 996 mm/year. A total of 3,902 mm of precipitation was measured and sampled during the whole period. The isotope ratios of precipitation samples are shown in Figure 2, with a classification of the samples as effective ($n = 224$) or non-effective ($n = 240$) for hydrological compartments according to the Thorntwaite-Mather water recharge model.

The isotope ratios of mobile soil water and groundwater samples are shown in Figure 3, where a scarcity of samples in late summer is apparent. At VP05 (but not at VP01), the scatter of groundwater $\delta^{18}O$ values was related to the dynamics of the water table (Figure 4 and Table 1): when the water table rose, the values tended to be most variable, with the isotope ratios ranging from the minimum to the maximum recorded for the time period studied. However, when the water table was at its lowest (-3.5 m), the isotope ratios tended to be less variable.

Stream discharge behaved differently in the two sampling periods (Figure 5). During the first one, there was a succession of wet and dry episodes, with several interludes without any runoff. The second period was wetter (annual precipitation = 996 mm) with sequences of intermediate events and the 5-minute highest discharge measured during the entire record ($2,619 \text{ m}^3\text{s}^{-1}$, equivalent to 404 mm d^{-1}).

The overall results of the ^{18}O analyses in the studied compartments are synthesized in Table 1. Mean simulated recharge was more depleted in heavy isotopes than precipitation because the simulated soil water balance is more adverse in summer and, in consequence, the recharge weights of summer-enriched isotopic sample signatures were usually lower than those in the colder seasons.

Some other differences between inputs and compartments are further presented in Table 2. The isotope ratios of precipitation was more depleted than any other compartment except for flow-weighted stream waters, although the only marginally significant differences were with groundwater at VP01 and deep groundwater at VP05. The isotope ratios for simulated recharge was even more depleted than for precipitation, but otherwise nearly all the differences between recharge and catchment compartments were either significant (soil waters and groundwaters at VP01) or marginally significant (groundwaters and time-weighted stream waters).

The volume-weighted ^{18}O and ^2H values of the precipitation waters drew a Local Meteoric Water Line (LMWL) with an adjusted determination coefficient $R^2=0.961$ ($p<0.001$):

$$\delta ^2H = 7.96 \delta ^{18}O + 13.3 \quad (10)$$

The sampled soil waters plotted reasonably close to the LMWL (Figure 6), although some of the more enriched samples taken at VL01 were slightly below the line, suggesting some fractionation due to evaporation. Stream water samples plotted close to the LMWL, except for the few more depleted samples that were clearly located below the LMWL, following the same trend as the precipitation waters (further information on precipitation isotopy at Can Vila can be found in Casellas *et al.*, 2019). Groundwaters showed no relevant displacement from the LMWL (not shown).

3.2 Assessing young water fractions

A first step in the study of the young water fraction is to calculate with Eq. (4) the seasonal amplitude and shift of the signature of precipitation. As stated in the Methods section, either the gross precipitation or the net precipitation obtained with a recharge model must be properly selected before the input isotope ratios are used. The comparisons shown in Table 2 reveal that the isotope ratios of the simulated recharge was more depleted than all the other hydrological compartments, so its use to explain the water partitioning should be discarded. The isotope ratios of gross precipitation was however more similar to the diverse compartments and can therefore be considered as more appropriate as input signature than the signature of the simulated recharge. The validity of this option was subsequently tested using the mass balance Eqs (1), (2) and (3).

the weighted average $\delta^{18}\text{O}$ value of precipitation from June to August was $-5.7 \pm 0.51 \text{ ‰}$, significantly different from the September to May signature, which was $-8.25 \pm 0.32 \text{ ‰}$. This allowed the analysis of the contribution of summer precipitation to groundwaters and runoff through the application of Eq. (1) to a period of three complete years (in order to avoid seasonally biased sampling). This equation give a value of $\rho=2.3$ for ground waters at VP05 and $\rho=1.2$ for flow-weighted stream waters. This indicates that precipitation in the period from June to August had contributions to ground- and stream waters somewhat higher than the rest of the year.

Yet, following a more detailed method, end-member splitting and mixing analyses using Eqs. (2) and (3) were applied to the data with the results shown in Table 3. Although the uncertainty is high, these results show (splitting) that summer precipitation is likely to contribute more to discharge (38 vs. 32%) and less to evapotranspiration (62 vs. 68%) than winter precipitation. In addition, discharge is composed (mixing) by summer and winter precipitations with percentages (33 and 67% respectively) similar to their relative

volumes (30 and 70%). These results point again to a relative contribution of summer precipitation to discharge similar or slightly higher than in the rest of the year.

Given these converging indicators, the precipitation-weighted isotope ratios were used for subsequent analysis of the seasonal variations, although the recharge-weighted signature was studied and reserved for some comparisons. The resulting implications are reviewed in the Discussion section.

The sine-wave fitting with Eq. (4) was subsequently applied to the isotope ratios of all eleven following compartments: precipitation (i), simulated recharge (ii), mobile soil water at VL01 (iii) and VL02 (iv), groundwater at VP01 (v), VP05(vi), level-weighted groundwater at VP05 (vii), groundwater at VP05 when the water table was shallow (viii) (0 to 2.25 m deep) and deep (ix) (deeper than 2.25 m), time-weighted stream water (x) and flow-weighted stream water (xi).

The results show a wide range of amplitudes and young water fractions, as calculated with Eq. (5) using precipitation A as Ap (Table 4). Attending to the resulting sinusoid amplitudes and F_{yw} obtained, these eleven hydrological compartments can be arranged with high statistical significance ($p < 0.001$, F-test) in four main groups: 1) mobile soil waters, flow-weighted stream water and shallow groundwater at VP05 had the highest F_{yw} and F_{yw}^* (0.207 to 0.344). 2) Level-weighted groundwater at VP05 had an intermediate F_{yw} (0.115). 3) Time-weighted stream water and bulk groundwater at VP05 had low but identifiable F_{yw} (0.062 to 0.078). Finally, 4) groundwater at VP01 and deep groundwater at VP05 had F_{yw} not significantly different from 0. This arrangement demonstrates a good relationship between flow-weighted stream F_{yw}^* and the more dynamic compartments of the catchment, clearly separated from the much lower rank of time-weighted stream F_{yw} and groundwaters.

3.3 Assessing the discharge sensitivity of young water fractions

For the Can Vila catchment, the flow-weighted young water fraction ($F_{yw}^* = 0.226 \pm 0.028$) was higher than the time-weighted young water fraction ($F_{yw} = 0.062 \pm 0.008$), suggesting a clear dependence of the young water fraction on discharge. To analyse this dependence, the time-weighted young water fractions for different quantiles of the flow regime were analysed as shown in Figure 7 (similar to Figure 7 in von Freyberg *et al.*, 2018), extending the range to portray the highest flows (exceeded 0.25% of time but by 16.6% of flow). This figure shows that F_{yw} increased with increasing discharge, from nearly 0 at the lowest discharge to nearly 1 for Q [?]24 mm d⁻¹, and underlines the usefulness of Eq. (8). This equation provides a basal (virtual for zero discharge) young water fraction that is indistinguishable from 0 ($F_0 = 0.024 \pm 0.028$) and rather large exponential sensitivity ($S_d = 0.056 \pm 0.01$ d mm⁻¹) parameters.

The wide range of F_{yw} values observed for the diverse flow quantiles might cast doubt on the potential role of the threshold age $\tau_{\psi\omega}$ that defines these fractions in the results. In order to analyse this question, Figure 8 shows the comparison of these time-thresholds obtained from Eqs. (6) and (7). This graph demonstrates that the thresholds did not play any role because they were consistently similar for the diverse flow quantiles analysed, although the uncertainty towards higher values strongly increased with increasing F_{yw} .

3.4 Analysing different sampling periods: role of precipitation forcing

Can Vila catchment data used for this work cover a period of over two years and another of one year. To analyse the variation of F_{yw}^* and S_d under different precipitation conditions, five 12-month time windows of both precipitation and stream waters were selected from the first period and compared with the last one-year period and the full record, as shown in the upper graph of Figure 9. Although both F_{yw}^* and S_d roughly increased with annual precipitation (upper graph), with the wettest year (996 mm) having the highest F_{yw}^* (0.34) and S_d (0.147 d mm⁻¹), the trend is highly irregular. Indeed, the driest year (671 mm) shows an intermediate F_{yw}^* (0.16) with a quite low S_d (0.011 d mm⁻¹), while the second wettest year (972 mm) shows a lower F_{yw}^* (0.12) but a higher S_d (0.035 d mm⁻¹).

When the coefficient of variation of discharge was used instead of precipitation as the forcing variable (lower graph in Figure 9), two very distinct conditions were shown: periods with low coefficient of variation of

discharge yielded moderate F_{yw}^* values and low S_d values whereas the period high coefficient of variation yielded high values of both metrics.

3.5 Role of sampling rate

All the results shown above on stream waters are based on the dynamic sampling design described in the Methods section. Nevertheless, most of the published F_{yw} studies are based on weekly-to-monthly sampling frequencies. As many authors agree that stream waters' transit time and F_{yw} results are affected by sampling rates, we used weekly spaced samples to calculate the main metrics describing F_{yw} and subsequently compared these results with the dynamic sampling results shown above.

The results show that both time-weighted and flow-weighted young water fractions using a weekly sampling frequency ($F_{yw} = 0.044 \pm 0.014$ and $F_{yw}^* = 0.103 \pm 0.033$) were significantly lower than results with dynamic sampling (Table 5).

Furthermore, the highest discharge sampled at Can Vila was 226 mm d^{-1} , a little more than half the maximum discharge recorded during the same period (404 mm d^{-1}). Therefore, as we know that F_{yw} approaching 1 are associated with the highest flows, the question arises as to whether the dynamic sampling implemented at Can Vila was sufficient to capture the real behaviour of F_{yw} dynamics. For this purpose, Eq. (8) was applied to simulate the $F_{yw}(Q)$ for every 5-minute discharge reading available for Can Vila during the sampling period and these simulated young water fractions were weighted with the corresponding discharge readings. The resulting flow-weighted young water fraction, as a measure of the virtually perfect sampling, which we name F_{yw}^{**} , was 0.304 ± 0.030 . The differences between the metrics obtained with the different sampling strategies and weighting are shown in Table 5, demonstrating that if F_{yw}^{**} is taken as the unbiased young water fraction, the F_{yw}^* estimates obtained with the dynamic and weekly sampling were underestimated by 25% and 66% respectively.

In order to obtain a graphic comparison of the behaviour of the different sampling methods, the 5-minute flow record was ordered from high to low discharges, and the corresponding time, flow and F_{yw}^* were cumulated for the 5-minute record and the two sampling designs (Figure 10). This compared the cumulated time (time-exceedance) of every record with the corresponding flow exceedance and young water fractions exceedance, making it easier to understand the results shown in Table 5. Both the cumulated 5-minutes flow and F_{yw}^* curves start close to 0 exceedance, showing that the highest recorded flows, in spite of their high value and F_{yw} being close to 1, occurred so rarely that the exceeded values for flow and F_{yw} are not relevant, which makes clear that the 5-minute record does indeed represent a thorough virtual sampling.

The highest discharges associated with the samples taken with the dynamic design exceeded 0.01% of time and represent 2.7% of flow and about 25% of the young water fraction (when a sufficient number of samples were taken for estimating F_{yw}^*). This means that about 25% of the young water fraction was missed for the assessment by the dynamic sampling design because this amount was associated with the higher discharges that were not sampled. Finally, the highest discharges associated with the samples taken with the weekly sampling rate are exceeded 0.6% of time and are associated with 17% of flow and about 66% of young water fraction, which was also lost for the assessment.

4. Discussion

Our results show a behaviour of young water fractions at the Can Vila catchment that is much more dynamic than those reported in any other catchment. The identification of this behaviour is attributable to the Mediterranean climatic setting, the small size of the catchment and the high sampling frequency available at this site for stream water tracer data.

An early outcome of this research was the need for an updated design of the discharge sensitivity of the young water fraction, adequate to cope with the non-linear behaviour of F_{yw} with discharge shown in Figure

7. This question was resolved previously, leading to the development of Eqs. (8) and (9), as described in Gallart *et al.* (2019).

Other results help improving the conceptualisation of the hydrological functioning of the Can Vila catchment and also contribute to revise questions raised by other researchers in this field as detailed in the introduction: the fate of rain water fallen in summer, the dependence of the young water fraction on precipitation forcing, the role of sampling frequency on catchment water turnover investigations and the young water fractions delivered by mountain catchments.

4.1 The recharge assumption

An unexpected result of this study was the finding that the isotopic signature of gross precipitation was adequate for analysing the turnover of surface and shallow groundwaters in the Vallcebre catchments, without any need for reducing the isotopic contribution of summer precipitation. In this catchment, summer is a period when evaporative demand is usually much higher than precipitation; flow in the streams strongly decreases and ceases in several reaches, saturated areas disappear and both soil water content and water table level decrease (Llorens *et al.*, 2018). Nevertheless, our results with Eqs (1), (2) and (3) indicate that summer precipitation is not rapidly evaporated in summer, nor does it experience more evapotranspiration than the precipitation during the rest of the year, but summer rain similarly contributes to the diverse hydrological compartments.

Thus, most of the water intensely evapotranspired in summer appears to be previously stored soil water. For groundwater it may be argued that, since bedrock at Can Vila is almost impervious, wet soils do not contribute much to percolation to the sampled aquifers because these are very shallow and located in the deeper horizons of soils, whereas summer precipitation also contributes to soil and ground water because it infiltrates into dry and often cracked soils. Using tritium, Gallart *et al.* (2016) found that MTTs were nearly 5 years in open shallow aquifers and nearly 7.5 years in base flows at Can Vila, revealing that these base flows are not only fed by the shallow aquifers but also partially fed by small deeper aquifers in the bedrock.

Indeed, base flows at Can Vila (exceeded 50% of time but by 95% of flow) showed a $\delta^{18}\text{O}$ values of -7.17 ± 0.016 significantly more depleted than the shallow groundwaters signature. This result points to the additional contribution to base flows by deeper more depleted groundwater that would be recharged mainly during wet winter periods. Using a modelling approach, a double aquifer system was also proposed for explaining base flows at Can Vila by Ruiz-Perez *et al.* (2016).

A study by Sprenger *et al.* (2019a) carried out during the second period analysed (2015) in a forested plot within the Can Vila catchment, showed that mobile soil water was consistently more enriched in heavy isotopes than ground and stream waters, a result analogous to ours in Table 2. However, water held in smaller soil pores and potentially used for transpiration by vegetation remained more depleted than any other compartment and was mainly refilled during winter. Our results in Table 3 show that $1,822 * 0.68 = 1,239$ mm of evapotranspired water was sustained from precipitation between September and May whereas only $766 * 0.62 = 475$ mm was sustained from precipitation between June and August, in convergence with Sprenger *et al.* (2019) findings but at the catchment scale.

Such findings had an impact on F_{yw} estimates in the diverse compartments studied. A hypothetical decreased contribution of summer precipitation would not only cause a shift in the mean input isotopic signature but also a reduction of its seasonal amplitude and, subsequently, an increase of the young water fractions. Figure 7 demonstrates that the young water fractions estimated at Can Vila for the highest flows are around 1, the maximum possible value. However, using the isotopic signature of the simulated recharge instead of that of the precipitation as A_p in Eq (5), the five points in Figure 7 that correspond to the highest flow regimes take inconsistent F_{yw} values greater than 1, although the excess does not reach statistical significance ($p=0.105$).

4.2 The role of precipitation forcing

As the young water fraction usually increases with discharge, wetter years or catchments may be expected to deliver higher young water fractions than dry ones, as found by several authors (Bansah & Ali, 2019; Clow *et al.* , 2018; Remondi *et al.* , 2019; von Freyberg *et al.* , 2018; Wilusz *et al.* , 2017; Zhang *et al.* , 2018). However, our results shown in Figure 9 make clear that annual precipitation is an insufficient driver for the behaviour of F_{yw}^* at Vallcebre, whereas the variation of discharge might better explain F_{yw}^* and particularly S_d . These results are consistent with those obtained by other authors on the role of temporal patterns or rainfall depths and intensities (von Freyberg *et al.* , 2018; Soulsby *et al.* , 2011; Wilusz *et al.* , 2017), and particularly with the modelling exercise of Remondi *et al.* . (2019) that suggested that catchments in semi-arid and Mediterranean climates have not only lower but also more variable young water fractions than catchments in more humid climates. Unfortunately, this kind of information on discharge sensitivity S_d for diverse periods or catchments is not yet available.

This result recalls the complexity of the runoff generation mechanisms at Can Vila already investigated by hydrometric and tracing methods and shows the need for further analyses at the event scale by combining the study of young water fractions with other event characteristics such as rainfall depth and intensity, antecedent conditions and new water contribution. This would contribute to investigate not only how the catchment behaves but also how it does work (Kirchner, 2019).

Yet, these results also cast doubt on the validity of single one-year F_{yw} investigations for characterizing catchment behaviour (Stockinger *et al.* , 2019) and support the idea that MTT and F_{yw} depends on climate forcing rather than on physiographic catchment characteristics (von Freyberg *et al.* , 2018; Hrachowitz *et al.* , 2009; Kirchner, 2019; Tetzlaff, Malcom & Soulsby, 2007; Remondi *et al.* , 2019).

As with other catchment characteristics driven by climate (e.g., precipitation, potential evapotranspiration, discharge), F_{yw} and its discharge sensitivity should, therefore, be compared between catchments through their long-term annual means and inter-annual variabilities.

4.3 The issue of sampling rate

The differences obtained for F_{yw} depending on the sampling rates confirm the warnings of several authors and particularly the results obtained by Stockinger *et al.* . (2016) as mentioned in the introduction section. Another relevant aspect is the inadequacy of the time-weighted young water fraction in a catchment with such variant discharge as Can Vila, even with the intensive sampling design implemented for this study.

This exercise shows that even an intensive sampling design such as the one implemented at Can Vila may underestimate F_{yw} if it is sensitive to discharge and flow rates have a high variability, because a relevant part of the young water fraction is associated to the higher, unsampled discharges. The method applied in the section 3.5 may be used to estimate the young water fraction F_{yw}^{**} that could be measured if a thorough sampling design (e.g., due to in-situ measurements) was implemented.

Investigations of the catchment F_{yw} should therefore analyse the flow duration curves, if detailed flow records are available. The relevant evaluating variable in this analysis is not the time exceedance of discharge values, but their flow exceedance, i.e. the fraction of flow associated to the higher discharges. Furthermore, if the S_d discharge sensitivity of F_{yw} has been investigated, F_{yw}^{**} can then be assessed to evaluate the quality of the metric obtained and to ponder the possible advantage of implementing a more detailed sampling design. Unfortunately, the weekly sampling performed at Can Vila is inadequate for this purpose, because the very low value of S_d obtained with this design greatly underestimates F_{yw}^{**} .

4.3 Young water fractions delivered by mountainous catchments.

With a mean topographic gradient of 25.6%, the F_{yw} predicted for Can Vila by the global assessment made by Jasechko *et al.* (2016) would be of about 0.091 with 90% confidence intervals about ± 0.061 . This range is fully adequate for the F_{yw} estimated at Can Vila using a weekly sampling rate (Table 5), the flow-weighted

estimate (0.103 +- 0.033) being more adjusted than the time-weighted one (0.044 +- 0.014). Yet, the time-weighted F_{yw} obtained at Can Vila using the dynamic sampling (0.062 +- 0.008) falls also well within the range of the global analysis by Jasechko et al. (2016).

Nevertheless, the flow-weighted F_{yw}^* estimate obtained at Can Vila with the dynamic sampling (0.226 +- 0.028) is not in line with the global relationship between topographic gradient and F_{yw} as shown by Jasechko et al (2016), while it is very close to the median (0.21) and a little lower than the mean (0.26) of the F_{yw} obtained by these authors for the full global sample of 254 rivers. Furthermore, the fully-sampled flow-weighted young water fraction F_{yw}^{**} estimated at Can Vila is 0.304 +- 0.030, a value that falls between the means obtained without weighting (0.26, 254 rivers) or by flow-weighting (0.34, 190 rivers) methods by Jasechko et al. (2016).

These comparisons recall the need to pay attention to the use of adequate sampling designs and weighting methods when catchments of diverse flow characteristics are compared. For a catchment with constant flow rate, any sampling rate and weighting method would yield the same young water fraction estimate. But the results obtained at Can Vila demonstrate that when the variability of flow rate is high, low frequency sampling and time-weighting designs will result in clearly underestimated young water fractions. It is not imprudent to speculate that mountainous catchments have, on average, more variable flow rates than those in flat areas of similar catchment area (Arnell, 1989). Thus, reports of lower young water fractions in mountain catchments could result from an underestimation of young waters due to too low sampling frequencies that miss covering the high young water fractions because of the flashy response in mountain catchments.

5 Conclusions

The application of the young water fraction approach to the Mediterranean Can Vila research catchment improved our understanding of the catchment response and shed light on some open questions, highlighting the value of small catchment research for the development of concepts and models.

In contradiction of the initial hypothesis, precipitation during summer contributes to evapotranspiration and runoff at a rate similar to that of precipitation during the rest of the year. Intense evapotranspiration during summer seems to mainly use soil water infiltrated previously, while summer rainfalls contribute to all the hydrological compartments. This means that the isotope concentrations analysed in the precipitation waters had to be weighted with the gross precipitation depths instead of those of “effective precipitation” for analysing the turnover of waters in the catchment.

The young water fraction is highly dynamic in the stream waters at Can Vila, varying between nearly 0 during low flows to nearly 1 during high runoff events. This dynamic is due to the combination of very high variability of discharge and a moderate discharge sensitivity of the young water fraction.

Furthermore, the young water fraction is also a highly varying catchment metric at Can Vila when different 12-month periods are investigated. Thus, the young water fraction turns out to be a metric associated much more closely with the characteristics of precipitation forcing during the studied period than with physiographic catchment characteristics. If used as a metric for catchment comparison, mean long-term means and variances should be used, just as they are used for other climate-driven traits such as annual precipitation or annual discharge.

The results confirmed that the sampling frequency is highly relevant to investigations of young water fractions (and by extension to MTT). At Can Vila, the dynamic sampling design (with sampling frequency between 30 minutes and 1 week) underestimated the young water fraction by 25% whereas the weekly sampling underestimated it by 66%. Water turnover studies should always be linked to the inspection of flow duration curves and, when possible, the method used in section 3.5 should be used to estimate the young water fraction associated to a virtual thorough sampling rate (F_{yw}^{**}), in order to assess the quality of the metric obtained and to ponder the possible advantages of implementing a more detailed sampling design.

Finally, more research is needed to generalize the young water fractions of mountain catchments, preventing a potential underestimation associated to an insufficient sampling frequency of their waters.

Acknowledgements

This research was supported by the projects TransHyMed (CGL2016-75957- R AEI/FEDER, UE) and MASCC- DYNAMITE (PCIN-2017-061/AEI) funded by the Spanish Ministerio de Ciencia, Innovacion y Universidades, as well as the grant SGR 2017 1643 funded by the Generalitat de Catalunya. C. Cayuela was the beneficiary of a predoctoral FPI grant (BES-2014-070609) funded by the Spanish Ministry of Economy and Competitiveness and the contribution by M. Sprenger was supported by the Deutsche Forschungsgemeinschaft (project no. 397306994).

We are grateful to G. Bertran, M. Roig-Planasdemunt and E. Sanchez for their support during field work at the Can Vila catchment, to J. Kirchner, J. von Freyberg and K. Beven for their comments, as well as to M. Eaude for his English style improvements.

Data availability statement

The data that support the findings of this study are available from Jerome Latron (jerome.latron@idaea.csic.es) upon reasonable request.

References

- Allen, S. T., Jasechko, S., Berghuijs, W. R., Welker, J. M., Goldsmith, G. R., and Kirchner, J. W. (2019a): Global sinusoidal seasonality in precipitation isotopes, *Hydrology & Earth System Sciences* , 23, 3423–3436, <https://doi.org/10.5194/hess-23-3423-2019>.
- Allen, S. T., Kirchner, J. W., Braun, S., Siegwolf, R. T. W., and Goldsmith, G. R.: (2019 b). Seasonal origins of soil water used by trees, *Hydrology & Earth System Sciences* , 23, 1199–1210, <https://doi.org/10.5194/hess-23-1199-2019>.
- Arnell, N. (1989) Humid temperate sloping land, *in* : Falkenmark, M., & Chapman, T. (Eds.). *Comparative hydrology: An ecological approach to land and water resources* . The UNESCO Press, Paris
- Benettin, P., Soulsby, C., Birkel, C., Tetzlaff, D., Botter, G., Rinaldo, A. (2017). Using SAS functions and high-resolution isotope data to unravel travel time distributions in headwater catchments. *Water Resources Research*, 1–15. <https://doi.org/10.1002/2016WR020117>.
- Bansah, S., & Ali, G. (2019). Streamwater ages in nested, seasonally cold Canadian watersheds. *Hydrological processes* , 33 (4), 495–511. <https://doi.org/10.1002/hyp.13373>
- Casellas, E., Latron, J., Cayuela, C., Bech, J., Udina, M., Sola, Y., Lee, K-O. & Llorens, P. (2019). Moisture origin and characteristics of the isotopic signature of rainfall in a Mediterranean mountain catchment (Vallcebre, eastern Pyrenees). *Journal of Hydrology* , 575, 767–779. <https://doi.org/10.1016/j.jhydrol.2019.05.060>
- Cayuela, C., Latron, J., Geris, J., & Llorens, P. (2019). Spatio-temporal variability of the isotopic input signal in a partly forested catchment: Implications for hydrograph separation. *Hydrological processes* , 33(1), 36–46. <https://doi.org/10.1002/hyp.13309>
- Clow, D. W., Mast, M. A., & Sickman, J. O. (2018). Linking transit times to catchment sensitivity to atmospheric deposition of acidity and nitrogen in mountains of the western United States. *Hydrological processes* , 32 (16), 2456–2470.
- Craig, H., (1961). Isotopic variations in meteoric waters. *Science* 133, 1702–1703.

<https://doi.org/10.1126/science.133.3465.1702>

von Freyberg, J., Allen, S. T., Seeger, S., Weiler, M., & Kirchner, J. W. (2018). Sensitivity of young water fractions to hydro-climatic forcing and landscape properties across 22 Swiss catchments. *Hydrol. Earth Syst. Sci* , 22 , 3841-3861.

Frisbee, M. D., Phillips, F. M., Campbell, A. R., Liu, F. & Sanchez, S. A. (2011). Streamflow generation in a large, alpine watershed in the southern Rocky Mountains of Colorado: is streamflow generation simply the aggregation of hillslope runoff responses? *Water Resources Research* , 47, W06512.

Gallart, F., Llorens, P. & Latron, J. (1994). Studying the role of old agricultural terraces on runoff generation in a small Mediterranean mountainous basin. *Journal of Hydrology* 159(1-4), 291-303. [https://doi.org/10.1016/0022-1694\(94\)90262-3](https://doi.org/10.1016/0022-1694(94)90262-3).

Gallart, F., Llorens, P., Latron, J., & Regues, D. (2002). Hydrological processes and their seasonal controls in a small Mediterranean mountain catchment in the Pyrenees. *Hydrology and Earth System Sciences* , 6 (3), 527-537. <https://doi.org/10.5194/hess-6-527-2002>

Gallart, F., von Freyberg, J., Valiente, M., Kirchner, J., Llorens, P. & Latron, J. (2019). Technical note: An improved discharge sensitivity metric for young water fractions, *Hydrology & Earth System Sciences Discussions* , <https://doi.org/10.5194/hess-2019-447>, in review.

Gallart, F., Roig-Planasdemunt, M., Stewart, M. K., Llorens, P., Morgenstern, U., Stichler, W., Pfister, L. & Latron, J. (2016). A GLUE-based uncertainty assessment framework for tritium-inferred transit time estimations under baseflow conditions. *Hydrological Processes* , 30(25), 4741-4760.

Hargreaves, G. H., & Samani, Z. A. (1982). Estimating potential evapotranspiration. *Journal of the irrigation and Drainage Division* , 108 (3), 225-230.

Hrachowitz M, Soulsby C, Tetzlaff D, Dawson JJC, Dunn SM, Malcolm IA. 2009. Using long-term data sets to understand transit times in contrasting headwater catchments. *Journal of Hydrology* 367: 237–248, DOI: 10.1016/j.jhydrol.2009.01.001

Jacobs, S., Rufino, M., Butterbach Bahl, K., Timbe Castro, E. P., Weeser, B., & Breuer, L. (2018). Assessment of hydrological pathways in East African montane catchments under different land use. *Hydrology and Earth System Sciences* , 22, 4981–5000. <https://doi.org/10.5194/hess-22-4981-2018>

Jasechko, S., Kirchner, J. W., Welker, J. M., & McDonnell, J. J. (2016). Substantial proportion of global streamflow less than three months old. *Nature Geoscience* , 9 (2), 126.

<https://doi.org/10.1038/NGEO2636>

Jasechko, S., S. J. Birks, T. Gleeson, Y. Wada, P. J. Fawcett, Z. D. Sharp, J. J. McDonnell & J. M. Welker (2014), The pronounced seasonality of global groundwater recharge, *Water Resources Research* , 50, 8845–8867, <https://doi.org/10.1002/2014WR015809>.

Jasechko, S., Wassenaar, L. I., & Mayer, B. (2017). Isotopic evidence for widespread cold-season-biased groundwater recharge and young streamflow across central Canada. *Hydrological processes* , 31 (12), 2196-2209. <https://doi.org/10.1002/hyp.11175>

Kirchner, J. W. (2016a). Aggregation in environmental systems—Part 1: Seasonal tracer cycles quantify young water fractions, but not mean transit times, in spatially heterogeneous catchments. *Hydrology and Earth System Sciences* , 20, 279–297. <https://doi.org/10.5194/hess-20-279-2016>

Kirchner, J. W. (2016b). Aggregation in environmental systems—Part 2: Catchment mean transit times and young water fractions under hydrologic nonstationarity. *Hydrology and Earth System Sciences* , 20, 299–328. <https://doi.org/10.5194/hess-20-299-2016>.

Kirchner, J. W. (2019). Quantifying new water fractions and transit time distributions using ensemble hydrograph separation: theory and benchmark tests. *Hydrology & Earth System Sciences* , 23 (1).

<https://doi.org/10.5194/hess-23-303-2019>

Kirchner, J. W. & Allen, S. T. (2020) Seasonal partitioning of precipitation between streamflow and evapotranspiration, inferred from end-member splitting analysis, *Hydrology & Earth System Sciences* , 24, 17-19.

<https://doi.org/10.5194/hess-24-17-2020>

Kirchner, J. W., Feng, X., Neal, C., & Robson, A. J. (2004). The fine structure of water-quality dynamics: the (high-frequency) wave of the future. *Hydrological Processes* , 18 (7), 1353-1359.

<https://doi.org/10.1002/hyp.5537>

Latron, J. & Gallart, F. (2007). Seasonal dynamics of runoff-contributing areas in a small Mediterranean research catchment (Vallcebre, Eastern Pyrenees). *Journal of Hydrology* 335 (1), 194-206.<https://doi.org/10.1016/j.jhydrol.2006.11.012>.

Latron, J. & Gallart, F. (2008). Runoff generation processes in a small Mediterranean research catchment (Vallcebre, Eastern Pyrenees). *Journal of Hydrology* , 358(3-4), 206-220.<https://doi.org/10.1016/j.jhydrol.2008.06.014>.

Latron, J., Llorens, P. & Gallart, F. (2009). The hydrology of Mediterranean mountain areas. *Geography Compass* 3 (6), 2045-2064.<https://doi.org/10.1111/j.1749-8198.2009.00287.x>.

Latron, J., Roig-Planasdemunt, M., Llorens, P. & Gallart, F. (2015). Combining stable isotopes and hydrometric data to investigate the stormflow response of a Mediterranean mountain catchment (Vallcebre Research Catchments, Spain), *Geophysical Research Abstracts* 17.

Latron, J., Soler, M., Llorens, P. & Gallart, F. (2008). Spatial and temporal variability of the hydrological response in a small Mediterranean research catchment (Vallcebre, Eastern Pyrenees). *Hydrological Processes* 22, 775-787. <https://doi.org/10.1002/hyp.6648>.

Llorens, P., Gallart, F., Cayuela, C., Planasdemunt, M. R., Casellas, E., Molina, A. J., Moreno-de-las-Heras, M., Bertran, G., Sanchez-Costa, E. & Latron, J. (2018). What have we learnt about Mediterranean catchment hydrology? 30 years observing hydrological processes in the Vallcebre research catchments. *Cuadernos de Investigacion Geografica / Geographical Research Letters* , (44), 475-502. <http://doi.org/10.18172/cig.3432>

Llorens, P., Latron, J., & Gallart, F. (1992). Analysis of the role of agricultural abandoned terraces on the hydrology and sediment dynamics in a small mountainous basin (High Llobregat, Eastern Pyrenees). *Pirineos*, 139, 27-46.

Lutz, S. R., Krieg, R., Muller, C., Zink, M., Knoller, K., Samaniego, L., & Merz, R. (2018). Spatial patterns of water age: Using young water fractions to improve the characterization of transit times in contrasting catchments. *Water Resources Research* , 54, 4767-4784.<https://doi.org/10.1029/2017WR022216>.

Maloszewski, P., Rauert, W., Stichler, W., & Herrmann, A. (1983). Application of flow models in alpine catchment area using tritium and deuterium data, *Journal of Hydrology* , 66, 319-330.[https://doi.org/10.1016/0022-1694\(83\)90193-2](https://doi.org/10.1016/0022-1694(83)90193-2)

Martin-Gomez, P., Barbeta, A., Voltas, J., Penuelas, J., Dennis, K., Palacio, S., Dawson, T.E. & Ferrio, J. P. (2015). Isotope-ratio infrared spectroscopy: a reliable tool for the investigation of plant-water sources?. *New Phytologist* , 207 (3), 914-927. <https://doi.org/10.1111/nph.13376>

McDonnell, J. J., & K. Beven (2014), Debates—The future of hydrological sciences: A common path forward? A call to action aimed at understanding velocities, celerities, and residence time distributions of the headwater hydrograph, *Water Resources Research* , 50, 5342-5350, <https://doi.org/10.1002/2013WR015141>.

- McGuire KJ, McDonnell JJ. (2006). A review and evaluation of catchment transit time modelling. *Journal of Hydrology* 330: 543–563. <https://doi.org/10.1016/j.jhydrol.2006.04.020>
- Neal, C., Reynolds, B., Rowland, P., Norris, D., Kirchner, J. W., Neal, M., Sleep, D., Lawlor, A., Woods, C., Thacker S., Guyatt, H., Vincent, C., Hockenhull, K., Wickham, H. & Guyatt, H. (2012). High-frequency water quality time series in precipitation and streamflow: From fragmentary signals to scientific challenge. *Science of the Total Environment* , 434, 3-12.
- Poyatos, R., Latron, J. & Llorens, P. (2003). Land use and land cover change after agricultural abandonment - The case of a Mediterranean mountain area (Catalan Pre-Pyrenees). *Mountain Research and Development* 23 (4), 362-368. [https://doi.org/10.1659/0276-4741\(2003\)023\[0362:LUALCC\]2.0.CO;2](https://doi.org/10.1659/0276-4741(2003)023[0362:LUALCC]2.0.CO;2).
- Remondi, F., Botter, M., Burlando, P., & Fatichi, S. (2019). Variability of transit time distributions with climate and topography: A modelling approach. *Journal of hydrology* , 569 , 37-50. <https://doi.org/10.1016/j.jhydrol.2018.11.011>
- Rubio, C.M., Llorens, P. & Gallart, F. (2008). Uncertainty and efficiency of pedotransfer functions for estimating water retention characteristics of soils. *European Journal of Soil Science* 59 (2), 339-347. <https://doi.org/10.1111/j.1365-2389.2007.01002.x>.
- Ruiz-Perez, G., Medici, C., Latron, J., Llorens, P., Gallart, F., & Frances, F. (2016). Investigating the behaviour of a small Mediterranean catchment using three different hydrological models as hypotheses. *Hydrological Processes* , 30(13), 2050-2062.
- Sole, A., Gallart, F., Pardini, G. & Aringhieri, R. (1992). How mudrock and soil physical properties influence badland formation at Vallcebre (Pre-Pyrenees, NE Spain). *Catena* 19 (3-4), 287-300. [https://doi.org/10.1016/0341-8162\(92\)90003-T](https://doi.org/10.1016/0341-8162(92)90003-T).
- Song, C., Wang, G., Liu, G., Mao, T., Sun, X., & Chen, X. (2017). Stable isotope variations of precipitation and streamflow reveal the young water fraction of a permafrost watershed. *Hydrological Processes* , 31 (4), 935-947. <https://doi.org/10.1002/hyp.11077>.
- Soulsby, C., Piegat, K., Seibert, J., & Tetzlaff, D. (2011). Catchment-scale estimates of flow path partitioning and water storage based on transit time and runoff modelling. *Hydrological Processes* , 25(25), 3960-3976.
- Soulsby, C., C. Birkel, J. Geris, J. Dick, C. Tunaley, & D. Tetzlaff (2015), Stream water age distributions controlled by storage dynamics and nonlinear hydrologic connectivity: Modeling with high-resolution isotope data, *Water Resources Research* , 51, 7759–7776, doi:10.1002/2015WR017888.
- Soulsby, C., C. Birkel, & D. Tetzlaff (2016), Characterizing the age distribution of catchment evaporative losses, *Hydrological Processes* , 30(8),1308–1312, doi:10.1002/hyp.10751.
- Sprenger, M., Llorens, P., Cayuela, C., Gallart, F., & Latron, J. (2019a). Mechanisms of consistently disjunct soil water pools over (pore) space and time. *Hydrology and Earth System Sciences* ,23 (6), 2751-2762. <https://doi.org/10.5194/hess-23-2751-2019>.
- Sprenger, M., Stumpp, C., Weiler, M., Aeschbach, W., Allen, S. T., Benettin, P. Dubbert, M., Hartmann, A., Hrachowitz, M., Kirchner, J.W., McDonnell, J.J., Orłowski, N., Penna, D., Pfahl, S., Rinderer, M., Rodriguez, N., Schmidt, M. & Werner, C.h, (2019b). The demographics of water: A review of water ages in the critical zone. *Reviews of Geophysics* , 57, 3: 800-834.
- Steenhuis, T. S., & Van der Molen, W. H. (1986). The Thornthwaite-Mather procedure as a simple engineering method to predict recharge. *Journal of Hydrology* , 84(3-4), 221-229. [https://doi.org/10.1016/0022-1694\(86\)90124-1](https://doi.org/10.1016/0022-1694(86)90124-1)
- Stewart, M.K., Morgenstern, U. & McDonnell, J.J. (2010). Truncation of stream residence time: how the use of stable isotopes has skewed our concept of streamwater age and origin. *Hydrological Processes* 24:

1646–1659. <https://doi.org/10.1002/hyp.7576>

Stewart, M.K., Morgenstern, U., McDonnell, J.J. & Pfister, L. (2012). The ‘hidden streamflow’ challenge in catchment hydrology: a call to action for stream water transit time analysis. *Hydrological Processes* 26: 2061–2066. <https://doi.org/10.1002/hyp.9262>

Stockinger, M. P., Bogena, H. R., Lucke, A., Diekkruger, B., Cornelissen, T., & Vereecken, H. (2016). Tracer sampling frequency influences estimates of young water fraction and streamwater transit time distribution. *Journal of hydrology* , 541 , 952-964. <http://dx.doi.org/10.1016/j.jhydrol.2016.08.007>

Stockinger, M. P., Bogena, H. R., Lucke, A., Stumpp, C., & Vereecken, H. (2019). Time variability and uncertainty in the fraction of young water in a small headwater catchment. *Hydrology and Earth System Sciences* , 23 (10), 4333-4347. <https://doi.org/10.5194/hess-23-4333-2019>.

Tetzlaff, D., Malcolm, I. A., & Soulsby, C. (2007). Influence of forestry, environmental change and climatic variability on the hydrology, hydrochemistry and residence times of upland catchments. *Journal of Hydrology* , 346(3-4), 93-111. Wilusz, D. C., Harman, C. J., & Ball, W. P. (2017). Sensitivity of catchment transit times to rainfall variability under present and future climates. *Water Resources Research* , 53, 10,231–10,256.

<https://doi.org/10.1002/2017WR020894>

Zhang, Q., Knowles, J. F., Barnes, R. T., Cowie, R. M., Rock, N., & Williams, M. W. (2018). Surface and subsurface water contributions to streamflow from a mesoscale watershed in complex mountain terrain. *Hydrological processes* , 32 (7), 954-967.

<https://doi.org/10.1002/hyp.11469>

Tables

Table 1: Main statistics of the ^{18}O analyses during the sampling periods. Precipitation and simulated recharge isotopic signatures were volume-weighted. Soil water was sampled with low suction lysimeters. Shallow and deep groundwater at VP05 refers to samples taken when water table levels were respectively shallower or deeper than 2.25 m

$\delta^{18}\text{O}$ ($^{\circ}/_{\text{00}}$)	Precipitation	Simulated recharge	Soil water VL01	Soil water VL02
Maximum	0.86	-0.10	-4.63	-4.78
Minimum	-19.12	-17.86	-8.58	-8.01
Mean	-7.15	-7.90	-6.66	-6.68
Std. Dev.	3.30	3.12	1.09	0.78
$\delta^{18}\text{O}$ ($^{\circ}/_{\text{00}}$)	Groundwater VP05	Groundwater VP05 shallow	Groundwater VP05 deep	Time-weighted Stream water
Maximum	-5.40	-5.40	-6.45	-5.50
Minimum	-7.99	-7.99	-7.99	-13.50
Mean	-7.01	-7.08	-6.93	-7.21
Std. Dev.	0.46	0.56	0.29	0.39

Table 2: Mean ^{18}O signatures and differences in diverse hydrological compartments respect to precipitation and simulated recharge waters. **Bold** differences are significant at the 1% level and *underlined* differences are significant at the 5% level (Student’s t test, two tails). VW means volume-weighted, TW means time-weighted and FW means flow-weighted statistics. Soil water was sampled with low suction lysimeters. Sh and dp groundwater at VP05 refers to samples taken when water table levels were respectively shallower or deeper than 2.25 m.

$\delta^{18}\text{O}$ ($^{\circ}/_{00}$)	Precipitation VW	Recharge VW	Soil VL01	Soil VL02	Ground VP01	Ground VP05	Ground VP05 sh	Ground VP05 dp	Stream TW
Mean	-7.24	-7.90	-6.66	-6.68	-6.81	-7.01	-7.08	-6.93	-7.21
Std. error	0.292	0.407	0.137	0.128	0.097	0.055	0.089	0.052	0.027
-		-0.66	0.58	0.56	0.43	0.23	0.16	0.31	0.03
Precipitation									
-			1.24	1.22	1.09	0.89	0.82	0.97	0.69
Recharge									

Table 3: Partition of seasonal precipitation into evapotranspiration and stream discharge obtained by the application of Eqs. (2) and (3) to three full years of data. P_x means seasonal precipitation, Q means total discharge, ET means total actual evapotranspiration. Relative P_x means the seasonal fraction of precipitation. Splitting P_{x-Q} and P_{x-ET} represent the fraction of seasonal precipitation that eventually becomes discharge and evapotranspiration respectively. Mixing Q_{-P_x} represents the fraction of discharge that derives from seasonal precipitation.

	June to August	September to May
Precipitation mm	766	1822
Relative P_x %	29.6	70.4
Splitting P_{x-Q} %	38 ± 14	32 ± 7
Splitting P_{x-ET} %	62 ± 23	68 ± 15
Mixing Q_{-P_x} %	33 ± 13	67 ± 15

Table 4: Characteristics of the sinusoid functions and young water fractions obtained by the application of Eq. (4) to all the studied water compartments. Ground VP05 level weighted means the results for groundwater at VP05 when the isotopic signature was weighted with the exponent of the water table level. Shallow ground water means when depth to the water table was between 0 and 2.25 m and deep ground water it was deeper than 2.25 m. A is the amplitude, k is the zero value and ϕ is the phase shift of the fitted sinusoid functions. F_{yw} is the young water fraction calculated with Eq. (5) using precipitation A as input amplitude (Ap). The abbreviation n. s. means that the value was not significantly different from 0. F_{yw} and F_{yw}^* respectively refer to time-weighted and flow-weighted young water fractions when estimated for stream waters. (1) denotes dimensionless variables.

Compartment	A ($^{\circ}/_{00}$)	k ($^{\circ}/_{00}$)	(days)	F_{yw} / F_{yw}^* (1)
Precipitation	3.01 ± 0.22	-7.99 ± 0.15	115.7 ± 3.5	-
Simulated recharge	2.35 ± 0.38	-7.81 ± 0.19	114.4 ± 3.8	-
Soil VL01	1.03 ± 0.18	-6.61 ± 0.11	148.2 ± 8.2	0.344 ± 0.064
Soil VL02	0.62 ± 0.18	-6.62 ± 0.12	137.6 ± 14.4	0.207 ± 0.062
Ground VP01	n. s.	-6.89 ± 0.11	-	n. s.
Ground VP05	0.24 ± 0.08	-7.02 ± 0.05	137.6 ± 14.4	0.078 ± 0.026
Ground VP05 level weighted	0.35 ± 0.10	-7.07 ± 0.06	144.6 ± 12.7	0.115 ± 0.033
Shallow Ground VP05	0.63 ± 0.15	-6.98 ± 0.08	150.4 ± 8.5	0.209 ± 0.051
Deep Ground VP05	n. s.	-6.92 ± 0.05	-	n. s.
Stream time weighted	0.19 ± 0.02	-7.21 ± 0.01	181.6 ± 5.8	0.062 ± 0.008
Stream flow weighted	0.68 ± 0.07	-7.43 ± 0.04	132.9 ± 3.6	0.226 ± 0.028

Table 5: Summary of the metrics obtained with the different sampling strategies and weighting methods. FW means flow-weighting, TW means time-weighting. Grey figures are not significantly different from 0. F_{yw}^{**} , F_{yw}^* and F_{yw} respectively refer to virtual sampling FW, dynamic and weekly sampling FW and dynamic and weekly sampling TW estimates of young water fractions. (1) denotes dimensionless variables.

Sampling and weighting methods	$F_{yw}^{**} / F_{yw}^* / F_{yw}$ (1)	F_0 (1)	S_d (d mm ⁻¹)
Virtual sampling FW	0.304 ± 0.030	-	-
Dynamic sampling FW	0.226 ± 0.028	0.024 ± 0.028	0.056 ± 0.010
Weekly sampling FW	0.103 ± 0.033	0.018 ± 0.046	0.018 ± 0.008
Dynamic sampling TW	0.062 ± 0.008	0.038 ± 0.007	0.035 ± 0.008
Weekly sampling TW	0.044 ± 0.014	-0.002 ± 0.015	0.025 ± 0.012

Figure legends

Figure 1: Map of the Can Vila catchment, showing the main land cover types and the location of the instruments and sampling sites used for this study.

Figure 2: Isotopic ratios of all the precipitation samples compressed into a single year period. Non-effective points represent the samples that were tentatively discarded as evapotranspired after the recharge model. Lines represent the seasonal variations according to the best fits of Eq(4).

Figure 3: Isotopic ratios of mobile soil and ground waters samples compressed into a single year period. Lines represent the seasonal variations according to the best fits of Eq(4), the dashed line showing that the amplitude A was not significantly different from 0 for VP01.

Figure 4: Variation of the isotopic ratios of ground water with water table level at VP05. The grey line separates the shallow and deep water levels analysed in Table 4.

Figure 5: Stream discharge (5-minute step) and isotopic ratios of stream waters during the recorded period.

Figure 6: $\delta^{2}\text{H}$ versus $\delta^{18}\text{O}$ plot of the precipitation, soil and stream waters, along with the Local Meteoric Water Line.

Figure 7: Variation in time-weighted young water fraction at the Can Vila catchment with increasing quantiles of the flow duration curve. The curve represents Eq. (8), using parameters obtained by fitting Eq. (9) to all the stream water $\delta^{18}\text{O}$ isotope values. Maximum sampled discharge was 226 mm d⁻¹. Vertical bars represent standard errors. (1) denotes a dimensionless variable. Reproduced from Gallart *et al.* (2019).

Figure 8: Time threshold for the definition of the young water fractions smaller than 1 shown in Figure 7, after Eqs. (6) and (7). Bars represent 90% confidence intervals. (1) denotes a dimensionless variable.

Figure 9: Flow-weighted young water fractions (\mathbf{F}_{yw}^*) and discharge sensitivities of young water fraction (S_d) for 6 one-year windows and the full record available at Can Vila. Q represents discharge. Bars represent standard errors. (1) denotes a dimensionless variable.

Figure 10: comparison between relative cumulated time, flow and \mathbf{F}_{yw}^* simulated applying Eq. (8) to the 5-minute step flow record, as well as the relative cumulated flows for the dynamic and weekly sampling records. The 1:1 line is shown as a reference for a uniform distribution.

Hosted file

Table 1.docx available at <https://authorea.com/users/293164/articles/421640-investigating-young-water-fractions-in-a-small-mediterranean-mountain-catchment-both-precipitation-forcing-and-sampling-frequency-matter>

Hosted file

Table 2.docx available at <https://authorea.com/users/293164/articles/421640-investigating-young-water-fractions-in-a-small-mediterranean-mountain-catchment-both-precipitation-forcing-and-sampling-frequency-matter>

Hosted file

Table 3.docx available at <https://authorea.com/users/293164/articles/421640-investigating-young-water-fractions-in-a-small-mediterranean-mountain-catchment-both-precipitation-forcing-and-sampling-frequency-matter>

Hosted file

Table 4.docx available at <https://authorea.com/users/293164/articles/421640-investigating-young-water-fractions-in-a-small-mediterranean-mountain-catchment-both-precipitation-forcing-and-sampling-frequency-matter>

Hosted file

Table 5.docx available at <https://authorea.com/users/293164/articles/421640-investigating-young-water-fractions-in-a-small-mediterranean-mountain-catchment-both-precipitation-forcing-and-sampling-frequency-matter>

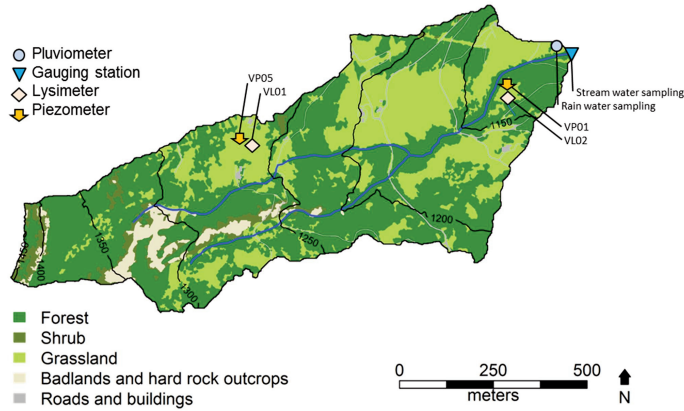


Figure 1: Map of the Can Vila catchment, showing the main land cover types and the location of the instruments and sampling sites used for this study.

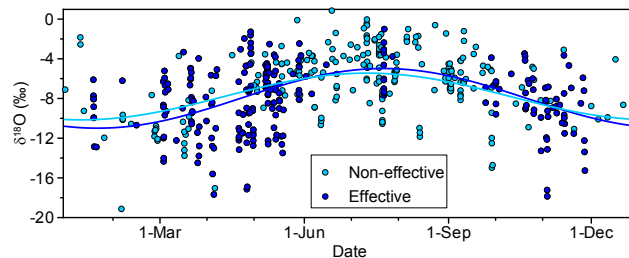


Figure 2: Isotopic ratios of all the precipitation samples compressed into a single year period. Non-effective points represent the samples that were tentatively discarded as evapotranspired after the recharge model. Lines represent the seasonal variations according to the best fits of Eq(4).

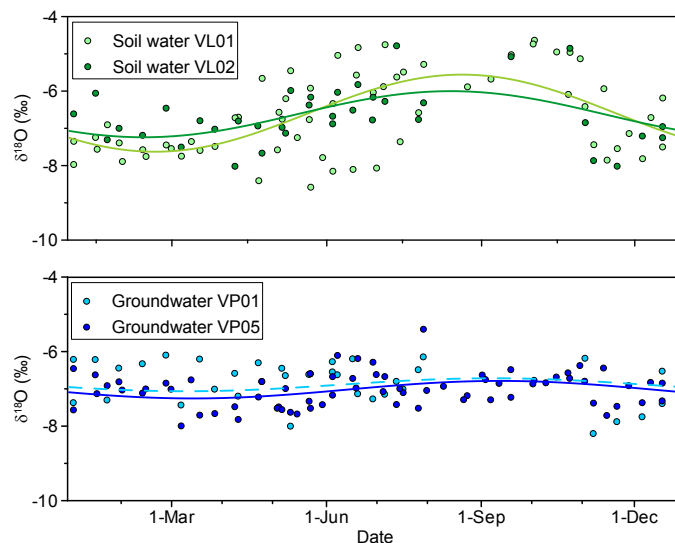


Figure 3: Isotopic ratios of mobile soil and ground waters samples compressed into a single year period. Lines represent the seasonal variations according to the best fits of Eq(4), the dashed line showing that the amplitude A was not significantly different from 0 for VP01.

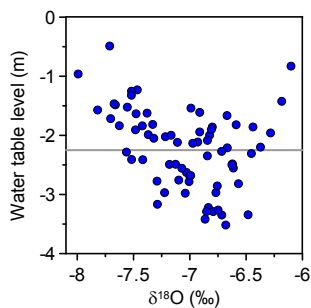


Figure 4: Variation of the isotopic ratio of ground water with water table level at VP05. The grey line separates the shallow and deep water levels analysed in Table 4.

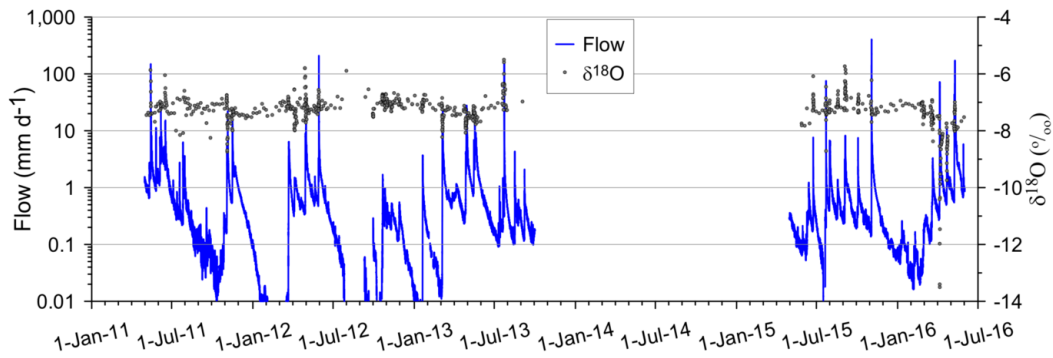


Figure 5: Stream discharge (5-minute step) and isotopic ratios of stream waters during the recorded period.

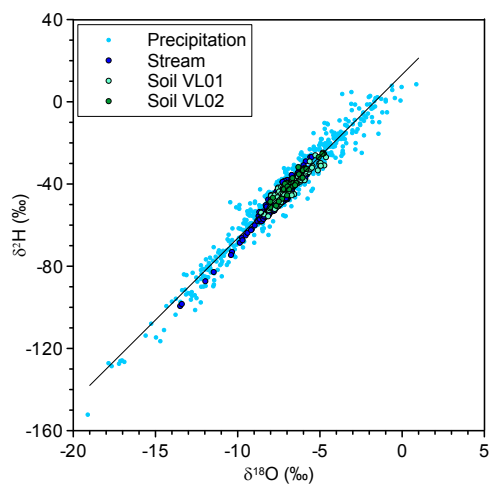


Figure 6: $\delta^2\text{H}$ versus $\delta^{18}\text{O}$ plot of the precipitation, soil and stream waters, along with the Local Meteoric Water Line.

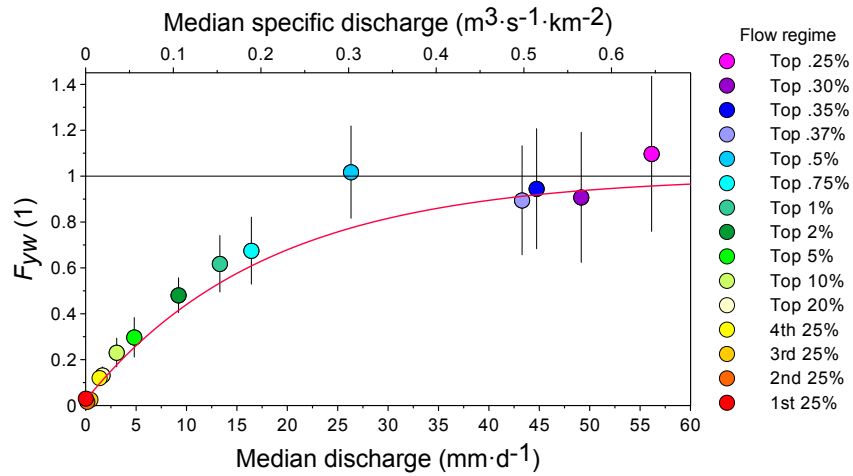


Figure 7: Variation in time-weighted young water fraction at the Can Vila catchment with increasing quantiles of the flow duration curve. The curve represents Eq. (8), using parameters obtained by fitting Eq. (9) to all the stream water $\delta^{18}O$ isotope values. Maximum sampled discharge was 226 mm d^{-1} . Vertical bars represent standard errors. (1) denotes dimensionless variables. Reproduced from Gallart et al. (2019).

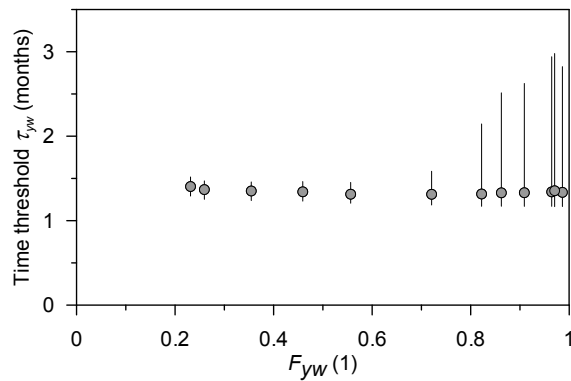


Figure 8: Time thresholds for the definition of the young water fractions smaller than 1 shown in Figure 7, after Eqs. (6) and (7). Bars represent 90% confidence intervals. (1) denotes dimensionless variables.

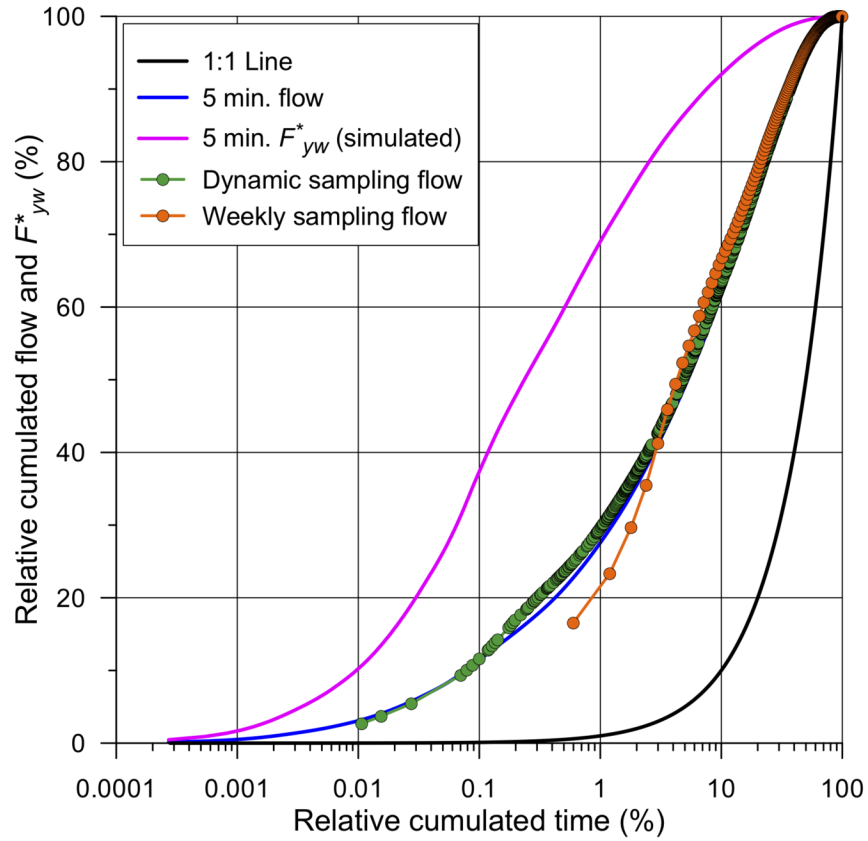


Figure 10: comparison between cumulated time, cumulated flow and cumulated F_{yw}^* simulated applying Eq. (8) to the 5-minutes step flow record, as well as the cumulated flows for the dynamic and weekly sampling records. The 1:1 line is shown as a reference for a uniform distribution.